hep-ph/0309110
SINP/TNP/03-31

Ultraviolet sensitivity of rare decays in nonuniversal extra dimensional models

Paramita Dey and Gautam Bhattacharyya

Saha Institute of Nuclear Physics, 1/AF Bidhan Nagar, Kolkata 700064, India

Abstract

We consider a nonuniversal five dimensional model in which fermions are localised on a four dimensional brane, while gauge bosons and a scalar doublet can travel in the bulk. As a result of KK number non-conservation at the brane-bulk intersection, the ultraviolet divergence does not cancel out in some physical observables. For example, the $B_d \to \ell^+\ell^-$ decay amplitude is linearly divergent, while B–$\bar{B}$ mixing amplitude is log divergent. We attempt to identify the exact source of this nonrenormalizability. We compare and contrast our results with those obtained in the universal five dimensional model where all particles travel in the extra dimension.

PACS Nos: 11.10.Kk, 12.60.-i
Key Words: Nonuniversal extra dimension, Kaluza-Klein tower, B decay

I Introduction

The idea that extra compactified space-like dimension may exist has caught the imagination of physicists working in phenomenology, string theory and cosmology alike. This had led to an important cross-road where perspectives from all the three avenues could melt, and as a result recent years have seen a huge boom of activity in this area. The possibility that the size of the extra dimension may be large [1], much higher than the Planck length of $\sim 10^{-33}$ cm, perhaps to the tune of $\text{TeV}^{-1} \sim 10^{-18}$ cm to be accessed by the standard model (SM) fields [2], or even as large as a millimeter where gravity or sterile neutrino could propagate [3, 4, 5, 6, 7], has brought the theory within the testable domain of the ongoing and future experiments.

In this paper, we consider a TeV scale extra dimensional model in which the SM fermions are four dimensional fields while the bosons can travel in the higher dimensional bulk [8]. Operationally, a higher dimensional theory can be described as an effective theory in four dimension which contains an infinite tower of four dimensional Kaluza-Klein (KK) modes of the higher dimensional fields. As a result, such effective theories are nonrenormalizable. In the conventional nonrenormalizable theories, at least at the tree level all processes are finite. But when we have more than one extra dimension, even the tree amplitude diverges. The theory then depends on two additional parameters – the compactification scale ($R^{-1} = M_c$) and the ultraviolet cut-off ($M_s = n_s/R$). For one extra dimension the tree amplitude is finite. But higher order processes are, in general, cut-off dependent.

In theories with only one extra dimension, another important observation [9] is that if the one loop diagrams involve a *single* summation over the KK modes then the theory is as well behaved as its zero mode counterpart. Then the total amplitude depends only on M_c and *not* on M_s. On the contrary, if there is more than one independent sum over KK modes inside a one loop integral, the total amplitude diverges.

The localisation of fermions on a four dimensional brane was motivated in [8] from a stringy perspective that chiral matters should be placed in the twisted sector while non-chiral states can travel in the bulk. We refer to this picture as the nonuniversal extra dimensional (NUED) model. In the present analysis we deal with a NUED model having only one extra dimension which is accessed only by the gauge bosons and the scalar doublet. Constraints on this class of models from electroweak observables were placed in [10]. The implications of this scenario in the context of $Z \to b\bar{b}$ decay and Kaon and B meson mixings have been studied in [9].

On the other hand, one may consider a situation in which all SM particles are allowed to travel in all available extra dimensions. These are called universal extra dimensional (UED) models. The simplest of this type, with only one extra dimension, was constructed and its implications to oblique electroweak parameters were studied in [11]. A detailed phenomenological implications, mainly related to FCNC processes, have been investigated in [12, 13, 14]. Implications of the UED scenario to $Z \to b\bar{b}$ decay has been examined in [15]. Other phenomenological implications in different variants of UED scenario have been studied in Refs. [16].

The core issue that distinguishes the ultraviolet behaviour of the UED and NUED models is the question of KK momentum conservation. Corresponding to every noncompact spatial dimension there is a conserved momentum. When that direction is compactified the momentum becomes discrete (n/R) but still remains a conserved quantity. The situation becomes tricky in the NUED models when, for example, a boson in the bulk couples to two fermions localised at the brane. The momentum in the extra dimension is not then conserved as a consequence of the breakdown of translational invariance at the brane. In other words, KK number does not remain conserved at the brane-localised interaction vertex. Any bulk interaction, however, does conserve KK parity. On the other hand, in the UED models all interactions do conserve KK number. In a loop diagram involving KK modes in the internal lines, the occurrence of a single summation or a multiple summation can be linked to the issue of KK number conservation or nonconservation. This constitutes the prime criterion to judge whether the theory would be well-behaved or ultraviolet sensitive. The one loop corrections in the UED model with *only one* extra dimension lead to finite results with R as the new physics parameter[1]. On the contrary, one loop corrections to a class of physical observables in NUED models with one extra dimension are vulnerable against unknown high scale physics, i.e., the results depend on n_s as well. The exact dependence indeed depends on the process concerned. When we go to higher loops, UED models also give rise to divergent results for physical observables. Indeed, the degree of divergence in NUED models is higher than that in UED models at any order.

In this context, we concentrate on flavour changing neutral current (FCNC) processes, in particular, the decay $B_d \to \ell^+\ell^-$. Such a decay can proceed through penguin and box graphs at leading order. The branching ratio is also GIM suppressed. We investigate how the SM penguin and box graphs are modified due to the presence of KK towers in the NUED framework. More specifically, we probe which are the specific diagrams and interaction vertices that are at the root of the ultraviolet sensitivity. We also revisit the B–$\bar{B}$ mixing and $Z \to b\bar{b}$ decay in the context of NUED scenario and agree with the results of [9]. We finally make a comment on the $t \to cZ$, $b \to s\gamma$, and $b \to s\ell^+\ell^-$ decays in such a scenario. We compare and contrast our results with those obtained in the UED scenario [12, 13, 14].

II The basic features of the NUED model

Here we set up our notations and recall the essential features of the NUED model.

1. The extra dimension (y) is compactified on a circle of radius $R = M_c^{-1}$ and y is identified with $-y$, i.e., it corresponds to an orbifold S^1/Z_2.

2. The fermions are four dimensional (4D) fields. They are all localised at the orbifold fixed point ($y = 0$).

[1] Any order loop corrections in UED models with more than one extra dimension are sensitive to the ultraviolet cut-off. The exact nature of the cut-off dependence depends on the number of extra dimensions [11]. Also, the degree of divergence may be different in different processes. The same is true in NUED models, only that the degree of divergence is higher.

3. The gauge bosons $A^M(x,y)$ and the scalar doublet $\phi(x,y)$ are five dimensional (5D) fields. The 5D fields can be Fourier expanded in terms of 4D KK fields as

$$A^\mu(x,y) = \frac{1}{\sqrt{2\pi R}}A^\mu_{(0)}(x) + \frac{1}{\sqrt{\pi R}}\sum_{n=1}^{\infty} A^\mu_{(n)}(x)\cos\frac{ny}{R}, \quad A^5(x,y) = \frac{1}{\sqrt{\pi R}}\sum_{n=1}^{\infty} A^5_{(n)}(x)\sin\frac{ny}{R}, \tag{1}$$

$$\phi^+(x,y) = \frac{1}{\sqrt{2\pi R}}\phi^+_{(0)}(x) + \frac{1}{\sqrt{\pi R}}\sum_{n=1}^{\infty} \phi^+_{(n)}(x)\cos\frac{ny}{R}, \quad \phi^-(x,y) = \frac{1}{\sqrt{\pi R}}\sum_{n=1}^{\infty} \phi^-_{(n)}(x)\sin\frac{ny}{R}. \tag{2}$$

Above, $x \equiv x^\mu$ (μ=0,1,2,3 denote the four non-compact space-time coordinates), y denotes the fifth (extra) compactified coordinate, and M =0,1,2,3,5. The fields $\phi^\pm_{(n)}(x)$ are the 4D KK scalar fields, $A^\mu_{(n)}(x)$ are the 4D KK gauge fields and $A^5_{(n)}(x)$ are the 4D KK scalar fields in the adjoint representation of the gauge group. The field $A^5(x,y)$ depends on sine of y to ensure its absence on the brane ($y = 0$).

4. A typical conventional bosonic 4D propagator is modified by the presence of KK towers in the following way:

$$(k_E^2 + M^2)^{-1} \longrightarrow \sum_{n=-\infty}^{\infty} (k_E^2 + M^2 + n^2/R^2)^{-1} = (\pi R/k'_E)\coth(\pi R k'_E), \tag{3}$$

where k_E is an Euclidean four momentum and $k'_E = \sqrt{k_E^2 + M^2}$. For large argument hyperbolic cotangent function goes like unity. Therefore, each modified propagator increases the degree of divergence by reducing one power of k_E in the denominator. This means that if a conventional diagram is log divergent in the ultraviolet limit, then KK towering for only one propagator makes it linearly divergent. If two propagators are modified, and the KK number for one is independent of the KK number of the other, i.e., the two sums can be independently carried out, then a logarithmically divergent diagram becomes quadratically divergent, and so on. However, if by virtue of KK number conservation, the KK indices of the two propagators are not independent, then the divergence will be less than quadratic.

5. In principle, the summation over KK number cannot go up to infinity. There should be an ultraviolet cutoff, which corresponds to the scale M_s at which unknown physics creeps in.

6. The KK number is not conserved when the interaction vertex is located at the brane, while any bulk interaction does conserve KK number.

Thus the parameters of the NUED model are R and M_s. We trade them for a ($\equiv \pi R M_W$) and n_s ($\equiv M_s R$).

III The decay $B_d \to \ell^+\ell^-$ in the SM

In the SM, the contribution to the $B_d \to \ell^+\ell^-$ decay comes from the penguin and box graphs. We work in the 't Hooft - Feynman gauge and we denote the would-be Goldstone bosons $\phi^\pm$ separately from the gauge bosons $W^\pm$. First, we consider the penguin part. The effective $Z\bar{b}d$ vertex is given by [17]

$$\Gamma^{Zbd}_\mu = -\frac{ig}{\cos\theta_W}\left(\frac{g^2}{16\pi^2}F_P^{\rm SM}\xi_t\right)\gamma_\mu P_L, \tag{4}$$

where $\xi_t = V_{tb}V^*_{td}$, and ($x_t \equiv m_t^2/M_W^2$)

$$F_P^{\rm SM} = \frac{x_t}{4}\Big[\frac{x_t-6}{x_t-1} + \frac{3x_t+2}{(x_t-1)^2}\ln x_t\Big]. \tag{5}$$

The penguin part of the decay amplitude is given by

$$\mathcal{M}_P^{\rm SM} = \frac{g^4}{64\pi^2 M_W^2}\xi_t\left(\frac{F_P^{\rm SM}}{2}\right)2t_{3\ell}\ (\bar{\ell}\ell)_{V-A}(\bar{b}d)_{V-A}. \tag{6}$$

Next we include the box contribution. This is dominated by $W^\pm$ exchanged graphs. The amplitude is given by

$$\mathcal{M}_B^{\rm SM} = \frac{g^4}{64\pi^2 M_W^2}\xi_t \left(\frac{F_B^{\rm SM}}{4}\right)(\bar{\ell}\ell)_{V-A}(\bar{b}d)_{V-A}, \tag{7}$$

where

$$F_B^{\rm SM} = \Big[\frac{x_t}{1-x_t} + \frac{x_t}{(1-x_t)^2}\ln x_t\Big]. \tag{8}$$

Combining the penguin and box contributions the total amplitude can be written as,

$$\mathcal{M}^{\rm SM} = \frac{g^4}{64\pi^2 M_W^2}\xi_t F^{\rm SM}(\bar{\ell}\ell)_{V-A}(\bar{b}d)_{V-A}, \tag{9}$$

where

$$F^{SM} = \left[\frac{F_B^{\rm SM}}{4} - \frac{F_P^{\rm SM}}{2}\right] = -\frac{x_t}{8}\left[\frac{x_t-4}{x_t-1} + \frac{3x_t}{(x_t-1)^2}\ln x_t\right]. \tag{10}$$

A discussion on why the penguin contribution is $(V-A)(V-A)$ type is now in order. The effective $Z\bar{b}d$ vertex has a pure $(V-A)$ form, while an effective $\gamma\bar{b}d$ vertex vanishes identically. So a photon cannot mediate the $B_d \to \ell^+\ell^-$ amplitude while a Z boson can. Furthermore, since one can write $J_Z^\mu = J_3^\mu - \sin^2\theta_W J_{\rm e.m.}^\mu$, only the t_3 dependent part of the Z coupling to final state leptons will contribute to the decay amplitude, while the coefficient of $\sin^2\theta_W$ in the amplitude would vanish identically.

Eq. (9) leads to the following expression for the decay width [18]:

$$\Gamma(B_d \to \ell^+\ell^-) = \frac{G_F^2}{\pi}\Big(\frac{\alpha}{4\pi\sin^2\theta_W}\Big)^2 m_B m_\ell^2 F_{B_d}^2 \xi_t^2 \Big[F^{\rm SM}\Big]^2, \tag{11}$$

where F_{B_d} is the decay constant.

IV Extra dimensional contributions to $B_d \to \ell^+\ell^-$

In the NUED model, the decay $B_d \to \ell^+\ell^-$ will again proceed via penguin and box contributions (see Figure 1). First, we consider the penguin graphs. Each such diagram will involve the KK towers of $W^\pm$ or $\phi^\pm$ as internal propagators (inside the loop), as well as the KK towers of Z boson or a photon as the external propagator (outside the loop) which couple to the final leptons. If we take the zero modes of both the internal and external lines, we get back the SM. Denoting the external propagator as V, one can write the effective $V\bar{b}d$ vertex as

$$\Gamma_\mu^V = -\frac{ig}{\cos\theta_W}\left(\frac{g^2}{16\pi^2}F_P^V\xi_t\right)\gamma_\mu P_L, \tag{12}$$

where V can be a zero mode Z boson ($Z_{(0)}$), or a KK Z boson ($Z_{(m)}$), or a KK photon ($\gamma_{(m)}$) (for the latter two cases $m \neq 0$). As we have mentioned in the context of SM calculation, the zero mode photon does not have any flavour changing effective vertex. But this is not true for a KK photon – we will discuss the reasons shortly. The F_P^V functions in Eq. (12) capture the KK loop dynamics when the indices of the internal KK propagators are summed over. They take appropriate forms $F_{Z_{(0)}}$, $F_{Z_{(m)}}$, or $(F_{\gamma_{(m)}}\sin\theta_W\cos\theta_W)$, depending on the nature of the external propagator V. In terms of these F functions the penguin amplitude in the NUED model can be written as

$$\mathcal{M}_P^{\rm NUED} = \frac{g^4}{64\pi^2 M_W^2}\xi_t(\bar{b}d)_{V-A}\left[\left(F_{Z_{(0)}} + F_{Z_{(m)}}\right)t_{3\ell}(\bar{\ell}\ell)_{V-A} - 2Q_\ell\sin^2\theta_W\left(F_{Z_{(m)}} - F_{\gamma_{(m)}}\right)(\bar{\ell}\ell)_V\right]. \tag{13}$$

We now discuss one by one the KK dynamics of the three F functions.

1. $Z_{(0)}$ *mediated penguins*: For each KK mode of the $W^{\pm}(\phi^{\pm})$ propagator, the observations are exactly similar to the case of the SM penguins. The ultraviolet divergence cancels mode by mode when all the graphs for the same KK mode are added up. In terms of a new variable $x_n = 1 + (n^2\pi^2/a^2)$, one can write the F function as

$$F_{Z_{(0)}} = 2\sum_{n=1}^{n_s} \frac{x_t}{4}\Big[\frac{6-x_t}{x_n-x_t} + \frac{x_n(-x_t+2)+4x_t}{(x_n-x_t)^2}\ln x_t + \frac{x_n(x_t-2)-4x_t}{(x_n-x_t)^2}\ln x_n\Big]. \tag{14}$$

It should be noted that for $n = 0$ the above function reduces to $F_P^{\rm SM}$ as expected. Since here we are interested to quantify the new physics part, we have not included $n = 0$ case in the summation. The sum is finite since for large n each term in the sum falls like $(\ln n/n^2)$. Clearly, the lighter KK modes dominate the sum.

2. $Z_{(m)}$ *mediated penguins*: Here the observations are very different from the SM case and there are quite a few issues that require attention. First of all, since the KK index of the external Z propagator is nonzero, the contributions from both the zero and nonzero modes of the $W^{\pm}(\phi^{\pm})$ loop propagators will have to be included within $F_{Z_{(m)}}$. Second, the ZWW, $ZW\phi$, and $Z\phi\phi$ vertices, which will appear in some of the penguin diagrams, do conserve KK parity. Hence, in such a diagram, say the one which involve $W^{\pm}$, instead of having two independent KK sums over the internal W indices plus another over the KK modes of the external Z, there will be altogether two (and not three) independent KK sums. This makes that particular diagram less divergent than what it would have been without the bulk KK number conservation.

Next comes the question whether the net divergence cancels or not. Curiously enough, here we encounter two sources of ultraviolet divergences. The first one is the conventional source which we encounter in the SM penguins too. From this perspective, as always, each penguin diagram is ultraviolet divergent. In the SM, for exmple, each penguin graph is logarithmically divergent. But in the present case, the degree of divergence is different for different diagrams. In this case, unlike in the SM, or for that matter in the case of $Z_{(0)}$ mediated penguins with KK loop propagators, when we add up all the amplitudes, the ultraviolet divergence does not mutually cancel and exhibit a $(\ln n_s)^2$ kind of cut-off dependence. The second source of ultraviolet divergence arises when the KK summations are carried over the so-called 'finite' part (i.e. ultraviolet finite for individual modes) for each diagram. Since each summation goes up to n_s, what finally emerges after adding up the KK-summed otherwise finite pieces from each diagram is a linearly divergent quantity (i.e. proportional to n_s). Obviously, this second source numerically dominates over the first one. The exact form of the F function in this case is not easily tractable in a compact elegant form (see Appendix A for individual expressions corresponding to each diagram). For all practical purposes, it can be expressed as

$$F_{Z_{(m)}} \sim a^2 n_s/\pi^2. \tag{15}$$

To understand the technical origin of this divergence, let us concentrate on some specific diagrams. Take any penguin amplitude in which the loop contains *two* bosons (WW, $W\phi$, or $\phi\phi$). For $Z_{(m)}$ mediated case the KK indices of the two internal bosons are independent; while, indeed, the index m of $Z_{(m)}$ is fixed by those two indices as a consequence of bulk KK number conservation. So there will be *more than one* KK sum (in this case, two) inside a one loop integral. This particular class of diagrams is finally responsible for the non-cancellation of net divergence. On the contrary, for $Z_{(0)}$ mediated amplitude, whatever be the internal lines inside the loop, there is always a single KK sum inside the integral, and the amplitude is convergent. This is exactly what we have seen just before.

3. $\gamma_{(m)}$ *mediated penguins*: A KK photon behaves differently from the standard (zero mode) photon in the sense that while the latter does not have any off-diagonal fermionic couplings, the former has. This is again due to the fact that the KK photonic penguin amplitudes which contain the three-boson bulk vertices do contain a double summation over the KK indices of the propagators involving the loop momentum. The F function can be expressed as

$$F_{\gamma_{(m)}} \sim a^2 n_s/\pi^2. \tag{16}$$

Indeed, there is a order one difference between the coefficients of $F_{Z_{(m)}}$ and $F_{\gamma_{(m)}}$ which we do not display here.

Now we turn our attention to the box contribution involving KK towers of $W^\pm$ and $\phi^\pm$. The box amplitude can be written as

$$\mathcal{M}_B^{\rm NUED} = \frac{g^4}{64\pi^2 M_W^2}\sum_i \xi_i \Big[\frac{F_B^{\rm NUED}}{4}\Big](\bar{b}d)_{V-A}(\bar{\ell}\ell)_{V-A}, \tag{17}$$

where

$$\begin{aligned} F_B^{\rm NUED} &= \sum_{n\neq 0}\sum_{m\neq 0}\Big[\Big(\frac{2x_n\ln x_n - x_n}{2(x_n-x_i)} - \frac{2x_m\ln x_m - x_m}{2(x_m-x_i)}\Big)\frac{1}{x_n-x_m} + \frac{2x_i\ln x_i - x_i}{2(x_n-x_i)(x_m-x_i)}\Big] \\ &\sim \ln n_s, \end{aligned} \tag{18}$$

where i runs over u, c, t quarks. The simultaneous occurence of zero modes is not included in the sum as that would correspond to the SM contribution which we take separately.

Combining the KK-summed penguin and box graphs together, one can calculate the relative change in the branching ratio $\mathcal{B}(B_d \to \ell^+\ell^-)$ as

$$\delta\mathcal{B}/\mathcal{B} = (\mathcal{B}^{\rm tot} - \mathcal{B}^{\rm SM})/\mathcal{B}^{\rm SM} \sim a^4 n_s^2/\pi^4. \tag{19}$$

What about the allowed choices of R and n_s? Measurements of Fermi constant and electroweak precision observables put a lower limit on R^{-1} to be order 1 TeV [10]. n_s should be restricted from two perspectives. First of all, n_s should not be too high such that $M_s = n_s/R$ gets very close to the scale where gravity becomes strong. Second, higher order loops in general would grow with higher powers of n_s. For example, we have checked that the most divergent two loop diagram for $B_d \to \ell^+\ell^-$ amplitude goes as $a^2 n_s^2 (\ln n_s)^2$. Calculation of the total two loop amplitude is beyond the scope of the present analysis. The only thing we can say is that n_s should not be so large that the enhancement due to powers of n_s at a given order overshoots the usual loop suppression at that order. Moreover, one must push up R^{-1} to a rather large value so that the scale (M_s) at which calculability is lost remains sufficiently high, yet reasonably below the scale of strong gravity.

V UED versus NUED scenarios

In this section we compare and contrast the renormalizability property of the UED and NUED models with only one extra dimension. In the former, all particles travel in the extra dimension, so the momentum along the extra coordinate is always conserved. Therefore, the KK number is conserved at every interaction point. Hence all the internal propagator lines inside a one loop diagram have the *same* KK number, hence a single summation, and the final amplitude is well-behaved with R as the only new physics parameter. On the other hand, in the NUED scenario, the KK number is not conserved at the brane though it is conserved in the bulk. The one loop propagators may involve more than one KK indices, hence a multiple KK summation inside the loop intergrals, and the final amplitude is ultraviolet divergent. This is the key issue behind the nonrenormalizability of the NUED model. The new physics parameters are both R and n_s.

In the UED model there are some additional interactions which are not present in the NUED model. Consider the scalars $W^5_{(n)}$, for example. Can they couple to standard zero mode fermions? They do, but in that case the other has to be a KK fermion in the same representation of the zero mode fermion but with a wrong chirality. The scalars $W^5_{(n)}$, $Z^5_{(n)}$ are in the adjoint representation of the gauge group and do not have any zero mode. It has been discussed in [12, 13, 14] how such scalars mix with the KK components of the doublet scalars to form three additional physical scalars $a^0_{(n)}$ and $a^\pm_{(n)}$. These additional scalars do not have any SM analog but their effects will have to be included in the loop calculations in the UED model. On the contrary, in the NUED model $W^5_{(n)}$ or $Z^5_{(n)}$ cannot couple to the brane localised SM fermions.

To provide more intuition into the impact of KK number conservation or non-conservation, we consider some examples, which will illustrate how the degree of divergence varies from process to process. We restrict our comparison only up to one loop order.

1. While we have analysed in detail why $B_d \to \ell^+\ell^-$ amplitude is linearly divergent in NUED models, the same decay amplitude is finite in UED models [12].

2. Consider the B_d–$\bar{B}_d$ or K_0–$\bar{K}_0$ mixing in the NUED model [9]. There are no bulk vertices, and the KK sums for the two boson propagators can be carried out independently. Each modified propagator increases the degree of divergence, and the final amplitude is log divergent. On the other hand, if one does this calculation in the UED model, the KK number being conserved at all vertices, there is only a single KK summation. Consequently, the final result is ultraviolet finite [15].

3. Consider the decay $Z \to b\bar{b}$. Since the external particles are all zero mode states, the loop propagators will involve a single KK index to be summed regardless of the UED or NUED nature of the model. In either case, the result is n_s independent [9, 15].

4. We have calculated the amplitude $t \to cZ$ in the NUED model. As expected, we obtain a cut-off independent amplitude since there is only a single KK summation. The numerical modifications are not significant.

5. In view of the arguments advanced above, it is not difficult to see that $b \to s\gamma$ amplitude is finite, but $b \to s\ell^+\ell^-$ amplitude is linearly divergent in NUED models. Both are finite in UED models [13].

VI Conclusions

The extra dimensional models are all nonrenormalizable due to the multiplicity of KK states. We know that one loop wavefunction renormalizations are linearly divergent leading to power law running of the couplings [19]. But when it comes to the calculation of physical observables, in some special cases there may be a cancellation between wavefunction renormalizations and vertex corrections leading to finite results (only at one loop). Our aim in this paper has been to identify the root cause of nonrenormalizability, in particular, the degree of divergence in different physical observables both in UED and NUED models. The crucial question is whether KK number is conserved or not. A summary of the situation is the following:

1. In the NUED model with only one extra dimension the tree level KK summed amplitude is finite. In the UED picture at the tree level there is no KK summation.

2. Next consider one loop corrections with one extra dimension. This constitutes the main thesis of our paper. While in the UED scenario the amplitude is finite, the NUED scenario suffers from ultraviolet sensitivity. In the latter framework, the $B_d \to \ell^+\ell^-$ amplitude provides a nice platform to examine the technical origin of the cut-off dependence as the KK indices are contained both in the 'internal' (i.e., inside the loop integral) and 'external' propagators. The interplay between the 'internal' and 'external' KK indices while being summed, and the number of such independent summations inside the loops, count to determine the degree of ultraviolet divergence. In the NUED scenario, (i) $B_d \to \ell^+\ell^-$ and $b \to s\ell^+\ell^-$ amplitudes are linearly divergent, (ii) B–$\bar{B}$ or K–$\bar{K}$ mixing is logarithmically divergent, while (iii) $Z \to b\bar{b}$, $t \to cZ$ and $b \to s\gamma$ decay amplitudes are finite. With the basic observations outlined in the previous sections, one can look at other processes and check their ultraviolet sensitivities.

3. Now consider two (or higher) loop corrections, again with only one extra dimension. The UED results are now divergent, while NUED results would be *more* divergent because the latter involves more KK summations.

4. Finally, take more than one extra dimension. Both UED and NUED models give divergent results at any order. As expected, the latter is more divergent than the former.

Acknowledgements

Both of us acknowledge hospitality of the Abdus Salam ICTP, Trieste, while a significant part of the work was being done. We thank E. Dudas and A. Raychaudhuri for reading the manuscript and valuable suggestions. We also thank T. Aliev and P.B. Pal for discussions. G.B.'s research has been supported, in part, by the DST, India, project number SP/S2/K-10/2001.

A Relevant loop integrals in the SM and NUED model

For the Z-penguin diagrams, the expressions for the effective $Z\bar{b}d$ vertex for the individual diagrams are given below (for each expression the loop propagators are written within square bracket).

$$\begin{aligned}
\Gamma^{\mu}[Wq_iq_i] &= -\frac{ig}{\cos\theta_W}\Big(\frac{g^2}{16\pi^2}\sum_i \xi_i\Big[2a_L^i I_3 + a_R^i x_i I_1\Big]\Big)\gamma_\mu P_L,\\
\Gamma^{\mu}[\phi q_iq_i] &= -\frac{ig}{\cos\theta_W}\Big(\frac{g^2}{16\pi^2}\sum_i \xi_i\frac{x_i}{2}\Big[a_R^i(2I_3-1/2) + a_L^i x_i I_1\Big]\Big)\gamma_\mu P_L,\\
\Gamma^{\mu}[WWq_i] &= -\frac{ig}{\cos\theta_W}\Big(\frac{g^2}{16\pi^2}\sum_i \xi_i\Big[-6\cos^2\theta_W I_4\Big]\Big)\gamma_\mu P_L,\\
\Gamma^{\mu}[\phi\phi q_i] &= -\frac{ig}{\cos\theta_W}\Big(\frac{g^2}{16\pi^2}\sum_i \xi_i\Big[\cos 2\theta_W\frac{x_i}{2} I_4\Big]\Big)\gamma_\mu P_L,\\
\Gamma^{\mu}[W\phi q_i] &= -\frac{ig}{\cos\theta_W}\Big(\frac{g^2}{16\pi^2}\sum_i \xi_i\Big[\sin^2\theta_W x_i I_2\Big]\Big)\gamma_\mu P_L,\\
\Gamma^{\mu}[Wq_i] &= -\frac{ig}{\cos\theta_W}\Big(\frac{g^2}{16\pi^2}\sum_i \xi_i\Big[-a_L^d I_5\Big]\Big)\gamma_\mu P_L,\\
\Gamma^{\mu}[\phi q_i] &= -\frac{ig}{\cos\theta_W}\Big(\frac{g^2}{16\pi^2}\sum_i \xi_i\Big[-a_L^d\frac{x_i}{2} I_5\Big]\Big)\gamma_\mu P_L.
\end{aligned} \tag{A.1}$$

For the zero mode Z propagators the I_i functions are given by,

$$\begin{aligned}
\int\frac{d^4k}{(2\pi)^4}2\sum_{n=1}^{n_s}\frac{1}{(k^2-m_i^2)^2(k^2-M_{W_n}^2)} &= -\frac{i}{16\pi^2M_W^2}I_1^{Z_{(0)}},\\
\int\frac{d^4k}{(2\pi)^4}2\sum_{n=1}^{n_s}\frac{k^\mu k^\nu}{(k^2-m_i^2)^2(k^2-M_{W_n}^2)} &= \frac{ig^{\mu\nu}}{16\pi^2}I_3^{Z_{(0)}},\\
\int\frac{d^4k}{(2\pi)^4}2\sum_{n=1}^{n_s}\frac{k^\mu}{(k^2-m_i^2)[(k-p)^2-M_{W_n}^2]} &= \frac{ip^\mu}{16\pi^2}I_5^{Z_{(0)}},\\
\int\frac{d^4k}{(2\pi)^4}2\sum_{n=1}^{n_s}\frac{1}{(k^2-m_i^2)(k^2-M_{W_n}^2)^2} &= -\frac{i}{16\pi^2M_W^2}I_2^{Z_{(0)}},\\
\int\frac{d^4k}{(2\pi)^4}2\sum_{n=1}^{n_s}\frac{k^\mu k^\nu}{(k^2-m_i^2)(k^2-M_{W_n}^2)^2} &= \frac{ig^{\mu\nu}}{16\pi^2}I_4^{Z_{(0)}}.
\end{aligned} \tag{A.2}$$

Above, we have used $M_{W_n}^2 = M_W^2 + (n/R)^2$. Since we take the SM contributions separately, to avoid any double-counting, we carry out the sum over the KK index n from 1 to n_s and multiply by an overall factor of 2, instead of performing the sum from $-n_s$ to $+n_s$.

When the Z propagator has nonzero KK mode, the propagator itself is modified as,

$$\frac{1}{M_Z^2} \longrightarrow 2\sum_{m=1}^{n_s} \frac{1}{M_Z^2 + n^2/R^2} \sim \frac{1}{M_Z^2}\left[2\sum_{m=1}^{n_s} \frac{a^2}{A\pi^2 m^2}\right], \tag{A.3}$$

where $A = (M_W/M_Z)^2$. The loop integrals are also modified, and the corresponding expressions for the I_i are given by,

$$\begin{aligned}
\int \frac{d^4k}{(2\pi)^4} 2\sum_{m=1}^{n_s} \frac{a^2}{A\pi^2 m^2} \sum_{n=-n_s}^{n_s} \frac{1}{(k^2 - m_i^2)^2 (k^2 - M_{W_n}^2)} &= -\frac{i}{16\pi^2 M_W^2} I_1^{Z_{(m)}}, \\
\int \frac{d^4k}{(2\pi)^4} 2\sum_{m=1}^{n_s} \frac{a^2}{A\pi^2 m^2} \sum_{n=-n_s}^{n_s} \frac{k^\mu k^\nu}{(k^2 - m_i^2)^2 (k^2 - M_{W_n}^2)} &= \frac{ig^{\mu\nu}}{16\pi^2} I_3^{Z_{(m)}}, \\
\int \frac{d^4k}{(2\pi)^4} 2\sum_{m=1}^{n_s} \frac{a^2}{A\pi^2 m^2} \sum_{n=-n_s}^{n_s} \frac{k^\mu}{(k^2 - m_i^2)[(k-p)^2 - M_{W_n}^2]} &= \frac{ip^\mu}{16\pi^2} I_5^{Z_{(m)}}, \\
\int \frac{d^4k}{(2\pi)^4} 2\sum_{m=1}^{n_s} \frac{a^2}{A\pi^2 m^2} \sum_{n=-n_s+m}^{n_s} \frac{1}{(k^2 - m_i^2)(k^2 - M_{W_n}^2)(k^2 - M_{W_{(n-m)}}^2)} &= -\frac{i}{16\pi^2 M_W^2} I_2^{Z_{(m)}}, \\
\int \frac{d^4k}{(2\pi)^4} 2\sum_{m=1}^{n_s} \frac{a^2}{A\pi^2 m^2} \sum_{n=-n_s+m}^{n_s} \frac{k^\mu k^\nu}{(k^2 - m_i^2)(k^2 - M_{W_n}^2)(k^2 - M_{W_{(n-m)}}^2)} &= \frac{ig^{\mu\nu}}{16\pi^2} I_4^{Z_{(m)}}.
\end{aligned} \tag{A.4}$$

Note that the limits of summation in the last two relations are so chosen that none of the KK numbers exceeds n_s. Also notice that in the last two integrals despite the presence of three KK propagators, KK number conservation ensures only two independent summation. This effectively reduces the degree of ultraviolet divergence.

Clearly, when all the KK indices are zero, the integrals correspond to the SM case.

References

[1] N. Arkani-Hamed, S. Dimopoulos and G. Dvali, Phys. Lett. B 429 (1998) 263 [hep-ph/9803315]; I. Antoniadis, N. Arkani-Hamed, S. Dimopoulos and G. Dvali, Phys. Lett. B 436 (1998) 257 [hep-ph/9804398].

[2] I. Antoniadis, Phys. Lett. B 246 (1990) 377.

[3] K. Dienes, E. Dudas and T. Gherghetta, Nucl. Phys. B 557 (1999) 25 [hep-ph/9811428].

[4] N. Arkani-Hamed, S. Dimopoulos, G. Dvali and J. March-Russell, Phys. Rev. D 65 (2002) 024032 [hep-ph/9811448].

[5] G. Dvali and A.Yu. Smirnov, Nucl. Phys. B 563 (1999) 63 [hep-ph/9904211].

[6] A. Ioannisian and A. Pilaftsis, Phys. Rev. D 62 (2000) 066001 [hep-ph/9907522].

[7] G. Bhattacharyya, H.V. Klapdor-Kleingrothaus, H. Pas and A. Pilaftsis, Phys. Rev. D 67 (2003) 113001 [hep-ph/0212169].

[8] A. Pomarol and M. Quirós, Phys. Lett. B 438 (1998) 255 [hep-ph/9806263]; I. Antoniadis, C. Muñoz and M. Quirós, Nucl. Phys. B 397 (1993) 515 [hep-ph/9211309].

[9] J. Papavassiliou and A. Santamaria, Phys. Rev. D 63 (2000) 016002 [hep-ph/0008151].

[10] See, for example, P. Nath and M. Yamaguchi, Phys. Rev. D 60 (1999) 116004 [hep-ph/9903298]; M. Masip and A. Pomarol, Phys. Rev. D 60 (1999) 096005 [hep-ph/9902467]; T.G. Rizzo and J.D. Wells, Phys. Rev. D 61 (2000) 016007 [hep-ph/9906234]; A. Strumia, Phys. Lett. B 466 (1999) 107 [hep-ph/9906266].

[11] T. Appelquist, H.-C. Cheng and B.A. Dobrescu, Phys. Rev D 64 (2001) 035002 [hep-ph/0012100].

[12] A. Buras, M. Spranger and A. Weiler, Nucl. Phys. B 660 (2003) 225 [hep-ph/0212143].

[13] A. Buras, A. Poschenrieder, M. Spranger and A. Weiler, hep-ph/0306158.

[14] D. Chakraverty, K. Huitu and A. Kundu, Phys. Lett. B 558 (2003) 173 [hep-ph/0212047].

[15] J.F. Oliver, J. Papavassiliou and A. Santamaria, Phys. Rev. D 67 (2003) 056002 [hep-ph/0212391].

[16] See, for example, T. Appelquist, Phys. Rev. D 64 (2001) 035002 [hep-ph/0012100]; K. Agashe, N.G. Deshpande and G.H. Wu, Phys. Lett. B 514 (2001) 309 [hep-ph/0105084]; T. Appelquist and B.A. Dobrescu, Phys. Lett. B 516 (2001) 85 [hep-ph/0106140]; F.J. Petriello, JHEP 0205 (2002) 003 [hep-ph/0204067]; K. Cheung and C.-H. Chou, Phys. Rev. D 66 (2002) 036008 [hep-ph/0205284]; T.Appelquist and H.-U. Yee, Phys. Rev. D 67 (2003) 055002 [hep-ph/0211023]; R. Mohapatra and A. Perez-Lorenzana, Phys. Rev. D 67 (2003) 075015 [hep-ph/0212254]. For collider searches, see, for example, T. Rizzo, Phys. Rev. D 64 (2001) 095010 [hep-ph/0106336]; C. Macesanu, C.D. McMullen and S. Nandi, Phys. Rev. D 66 (2002) 015009 [hep-ph/0201300]; Phys. Lett. B 546 (2002) 253 [hep-ph/0207269]; H.-C. Cheng, Int. J. Mod. Phys. A 18 (2003) 2779 [hep-ph/0206035].

[17] G. Buchalla and A. J. Buras, Nucl. Phys. B 400 (1993) 225.

[18] G. Buchalla, A. J. Buras and M. E. Lautenbacher, Rev. Mod. Phys. B 68 (1996) 1125 [hep-ph/9512380].

[19] K. Dienes, E. Dudas and T. Gherghetta, Nucl. Phys. B 537 (1999) 47 [hep-ph/9806292]; Phys. Lett. B 436 (1998) 55 [hep-ph/9803466].

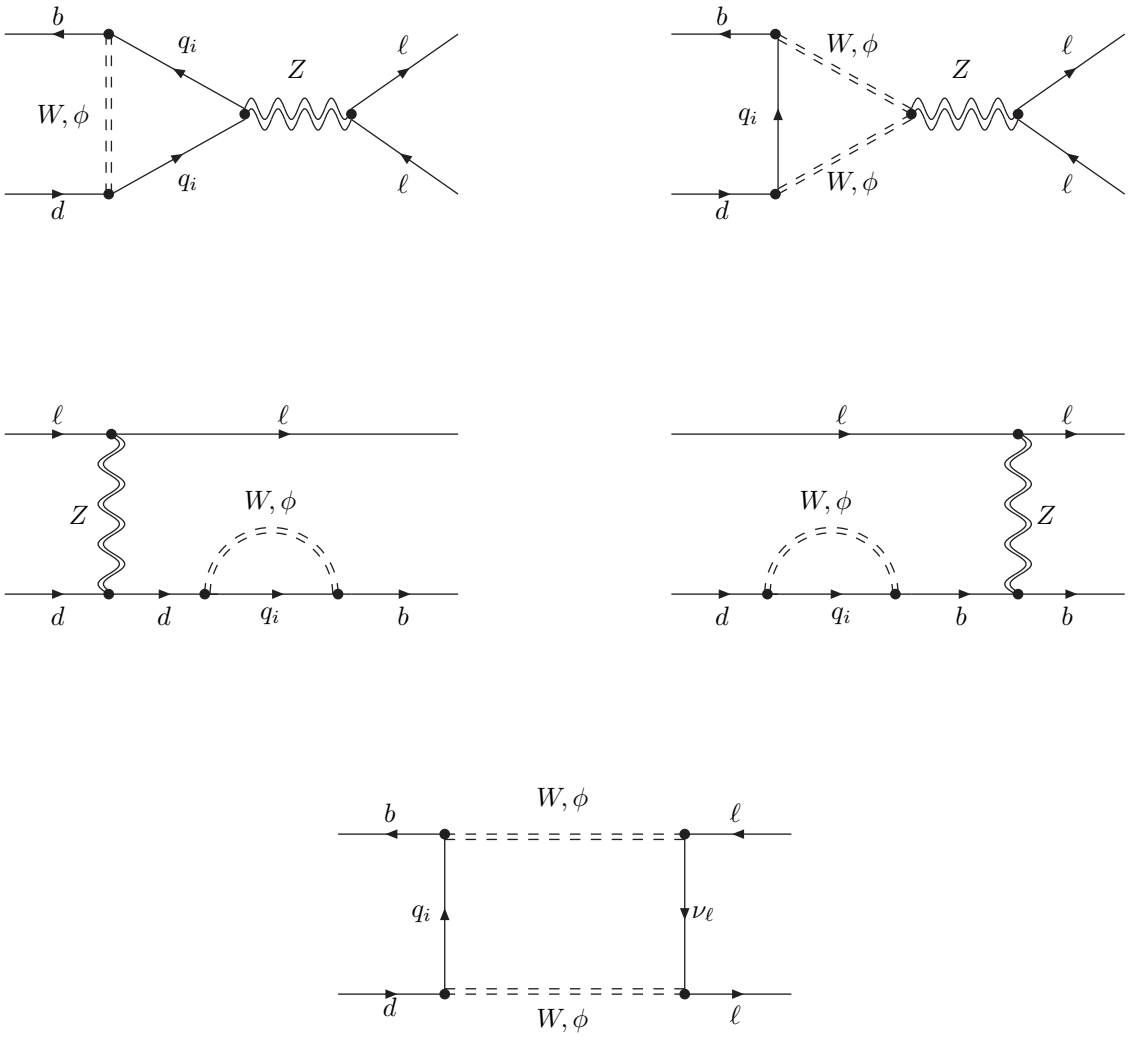

Figure 1: The Feynman graphs contributing to $B_d \to \ell^+\ell^-$. The bosons are shown as double lines (dashed and wavy) which can have zero or non-zero KK modes.